Directional conductivity in SWNT-collagen-fibrin composite biomaterials through strain-induced matrix alignment

Christopher M. Voge, Mihalis Kariolis, Rebecca A. MacDonald, Jan P. Stegemann
Department of Biomedical Engineering, Rensselaer Polytechnic Institute, Troy, NY 12180

Received 13 February 2008; accepted 14 February 2008
Published online 21 April 2008 in Wiley InterScience (www.interscience.wiley.com). DOI: 10.1002/jbm.a.32029

Abstract: Composite biomaterials incorporating fibroblast cells, collagen Type I, fibrin, and 2 wt % carboxylated SWNT were created, and their properties were compared with similar control constructs without SWNT. Alignment of the matrix was stimulated by application of 8% cyclic strain for three 12-h periods over three days. All constructs underwent cell-mediated gel compaction to 15–20% of their initial volume, which was not affected by SWNT loading. Mechanical strain increased the rate of compaction, and strained constructs were significantly more compacted than unstrained controls by day 3. Cell viability and morphology were similar in both control and SWNT-loaded constructs, but unstrained samples exhibited a more stellate appearance with more numerous cellular projections. Application of mechanical strain caused clear alignment of both the cells and matrix in the direction of the applied strain. Bioimpedance measurements showed that SWNT loading increased the electrical conductivity of composite constructs, and that mechanically-induced alignment of the matrix/SWNT caused a further increase in conductivity. These results demonstrate that SWNT can be used to augment the electrical properties of 3D protein hydrogels, and that anisotropy in the matrix further enhances these properties. Such electrically conductive biopolymers may have a variety of applications in tissue engineering and biosensor development. © 2008 Wiley Periodicals, Inc. J Biomed Mater Res 86A: 269–277, 2008

Key words: biomaterials; carbon nanotubes; collagen gel; fibrin gel; electrical conductivity; bioreactor; nanotechnology

INTRODUCTION

The combination of materials science with recent advances in nanotechnology is stimulating the development of new types of biomaterials for a variety of applications. The field of tissue engineering has benefited from this convergence in important ways. New nanostructured and composite materials have been created that use the unique properties of specific nanoparticles to recreate or improve the function of engineered tissues (for recent reviews, see e.g. ref. 1, 2) Our laboratory has been developing composite biomaterials that combine the self-assembly features of structural extracellular matrix (ECM) proteins with the unique mechanical and electrical properties of single-walled carbon nanotubes (SWNT). Our goal is to create electrically conductive biopolymers for use as scaffolds in tissue engineering and other applications.

Correspondence to: J.P. Stegemann; e-mail: stegemann@rpi.edu

Contract grant sponsor: New York State Office of Science, Technology and Academic Research

Carbon nanotubes have been extensively studied for use in biomaterials applications.[3] SWNT in particular have been explored in applications such as enhancing the properties of synthetic[4] and natural[5] polymer composites, as well as creating scaffolds for cellular growth and differentiation.[6,7] A key property of certain SWNT structures is their ability to efficiently conduct electricity along their major axis, while acting as electrical insulators across their short axis.[8] This electrical anisotropy makes SWNT very attractive as fiber additives in polymeric composites designed to carry current.[9] However, the full benefit of these nanofibers is obtained only when they can be directionally aligned within the composite material. Such anisotropy has been achieved in certain synthetic polymer systems,[10,11] but it has been more difficult to create similar materials using biologically relevant matrices.

Many ECM proteins undergo well characterized self-assembly processes that combine nanometer-dimension molecules into higher order fibrillar structures. Collagen Type I and fibrin are two such proteins, which have been used previously to make protein composite materials.[12,13] Collagen is a main structural ECM protein in many tissues, whereas

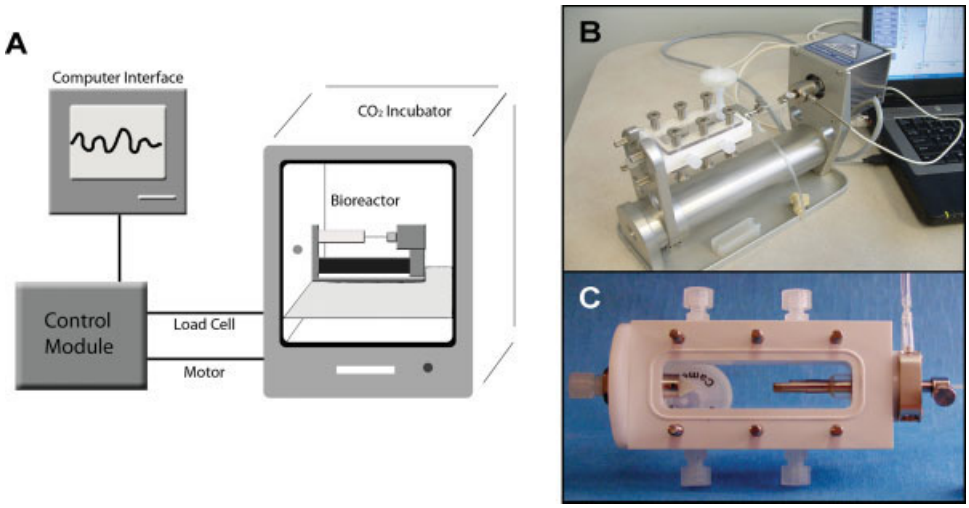

Figure 1. A) Schematic of bioreactor system showing computer control of stimulator and placement of bioreactor in incubator. B) Image of stimulator and bioreactor chamber assembly. C) Detail of bioreactor assembly showing actuator. [Color figure can be viewed in the online issue, which is available at www.interscience.wiley.com.]

fibrin fibers constitute the main structural component of blood clots. These proteins can be solubilized and then reconstituted in the presence of living cells, forming 3D fibrillar hydrogel constructs with cells embedded directly in the matrix. An advantage of such materials as tissue engineering scaffolds is that cells can recognize and bind to the matrix, and subsequently remodel it in response to a variety of environmental stimuli. Several different methods of inducing ECM alignment have been developed, including directed cellular compaction,[14,15] compressive[16] and tensile[17,18] strain, fluid flow,[19,20] and electrical[21] and magnetic[22] stimulation.

In our previous work, we have shown that carboxylated SWNT can be incorporated into 3D collagen matrices while maintaining robust gel compaction and cell viability.[23] In addition, we have shown that even randomly oriented SWNT-collagen composite materials have improved electrically conductivity, relative to pure collagen matrices.[24] In the present study, we have harnessed the self-assembly and mechanically-induced reorganization of 3D protein matrices to directionally align SWNT-collagen-fibrin matrices, with the goal of using anisotropy to increase the electrical properties of these materials. Directionally conductive engineered tissues may have application in a variety of fields, including stem cell biology, cardiac and neural tissue engineering, and biosensor development.

MATERIALS AND METHODS

Cell culture

Human Neonatal Dermal Fibroblasts (HNDFb) (Cambrex, Cambridge, MA), were cultured for use in SWNT-collagen-fibrin constructs. This cell type was chosen as a model because protein hydrogel compaction by HNDFb is a well characterized and consistent process. The cells were cultured in DMEM, supplemented with 10% fetal bovine serum (FBS, HyClone, Logan, UT), 2 mM L-glutamine (Cellgro, Herndon VA), 100 U/mL penicillin (Cellgro), and 100 μg/mL streptomycin (Cellgro). Cells were incubated at 37°C in 5% CO_2, growth medium was changed every 2 days and cells were harvested at 80–90% confluence between passages five and nine with 0.05% trypsin (Cellgro). Cell numbers were calculated using a Multisizer 3 (Beckman Coulter, Miami, FL) at cell diameters between 10 and 30 μm.

Uniaxial strain bioreactor

The bioreactor system was designed and built by Tissue Growth Technologies (TGT LigaGen™, Minnetonka, MN). The schematic of the system is presented in Figure 1A. A computer interface sends programmed wave forms to the control module, which in turn controls the mechanical stimulator. Figure 1(B) shows and image of the stimulator and construct chamber, and Figure 1(C) shows a close-up of the construct chamber and internal actuator. The stimulator is comprised of a linear actuator, load cell, and a mount for construct chambers, as shown schematically in Figure 2A. The entire assembly was maintained under standard cell culture conditions in a large incubator. Data acquisition was performed through the TGT software interface allowing for precise control of system parameters including displacement and cyclic waveforms. The individual bioreactor sample chambers [Fig. 2(B)] contained a removable mold for seamless transfer from sample preparation to mechanical stimulation. The ends of each chamber well contained porous polypropylene anchors that fixed the tissue constructs in place during initial gel compaction and successive mechanical stimulations. Luer ports provided gas exchange through sterile filters and a simple method for the replacement of growth medium. Each

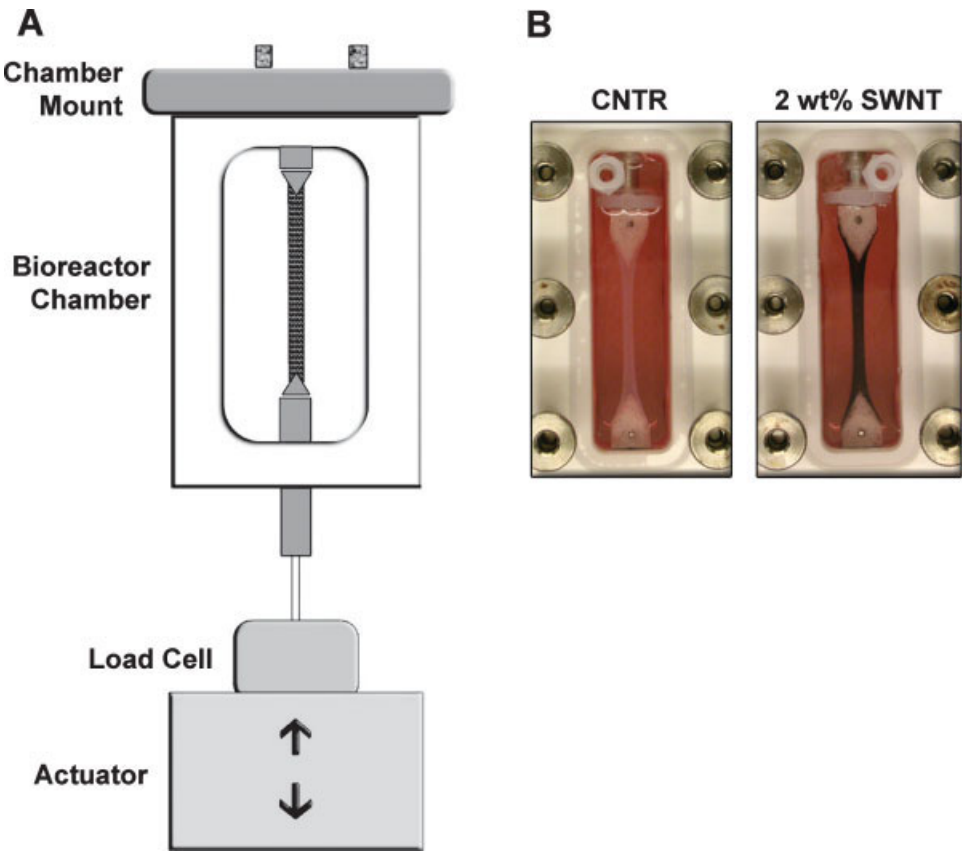

Figure 2. A) Schematic of bioreactor chamber and stimulator set-up. B) Images of constructs containing only collagen-fibrin (CNTR) and 2 wt % SWNT in collagen-fibrin (SWNT) mounted in bioreactor chamber. [Color figure can be viewed in the online issue, which is available at www.interscience.wiley.com.]

chamber was pre-assembled and steam sterilized at 121°C for 20 min before construct preparation.

Construct preparation and mechanical stimulation

Construct solutions consisted of HNDFb combined with 5× concentrated DMEM, SWNT solution, 10% fetal bovine serum, bovine thrombin and acid solubilized Type I bovine collagen (4.0 mg/mL, MP Biomedicals, Solon, OH). In order to maintain a physiologic pH, the solution was buffered with 0.1*M* NaOH. HNDFb were collected by trypsinization, counted, centrifuged, and added to the solution at a concentration of 1.0*M* cells/mL. The SWNT were functionalized as described previously[24] and sonicated in deionized water for 7–10 min to create homogenous solutions at 2.0 wt %. Control constructs did not contain SWNT but rather the same volume of deionized water. All mixing was done on ice to prevent gelation. The final solution was pipetted evenly into each bioreactor chamber mold, and chambers then were incubated at 37°C to allow for gelation and development of the cell-seeded construct. After 12 h of gelation the constructs had adhered to the porous polypropylene and the chamber molds were removed. The constructs were submerged in cell culture medium supplemented with ε-amino-caproic acid (ACA, Sigma) to inhibit the fibrolytic degradation of the fibrin. Strained samples were cyclically distended at 8% strain for three 12 h periods. The first period occurred after the initial 12 gel compaction period and strained samples were kept at 0% strain for the intervening periods. This strain protocol (i.e. strain-rest-strain-rest-strain) was used to allow the hydrogels to compact between strain regimens. Static samples were incubated while fixed in place over

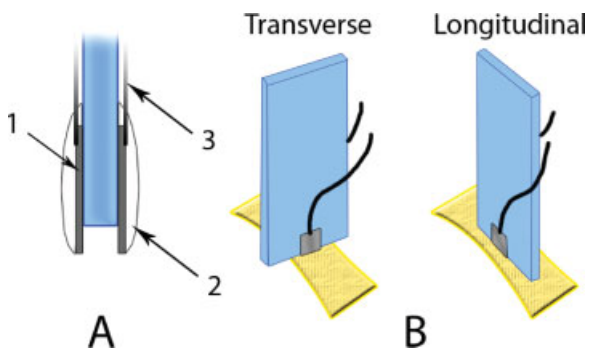

Figure 3. A) Schematic of 2-point silver chloride electrode used to measure bioimpedence of constructs, showing silver sheet (1), silicone insulation (2) and silver lead wires (3). B) Schematic showing method used to measure transverse and longitudinal electrical properties of constructs. [Color figure can be viewed in the online issue, which is available at www.interscience.wiley.com.]

the 3-day culture period. Culture medium for all samples was exchanged once daily and on day 3 the constructs were removed for analysis.

Construct characterization

Gel compaction was measured for all of the constructs every 12 h starting at day 1 and including day 3. Digital photos were taken and surface areas were measured using ImageJ 1.34s software (W. Rasband, NIH, Freeware). Compaction was assumed to be uniform so that we could calculate construct thicknesses and volumes. Rates of compaction were also compared for 12 h time periods between static and strained samples.

To analyze the structure of the ECM, both static and strained constructs were examined via scanning electron microscopy (SEM, Zeiss, Thornwood NY). Samples were prepared by fixation in 4% glutaraldehyde for 1 h, a dehydration series in ethanol (30, 50, 70, 90, 2× 95, 2× 100%), and were critically point dried in a Autosamdri-851 (Tousimis Corp., Rockville, MD). Dried samples were mounted on Al stubs and sputter coated in platinum before being analyzed.

Confocal microscopy (Zeiss LSM510Meta, Thornwood, NY) was used to analyze cell viability and morphology. Cell viability was quantified using a vital dye kit (Molecular Probes, Eugene OR) with calcein and ethidium homodimer on day 3. Images were obtained with a 10× objective to thoroughly estimate cell viability throughout the tissue constructs. Individual cells were segmented and counted with ImageJ plugins (WCIF, Toronto, ON) to quantify percent viability. Actin cytoskeleton and nuclear staining was also performed with Alexa Flour® 488 phalloidin (Invitrogen, Carlsbad, CA) and ethidium homodimer. Cell morphology was assessed qualitatively by examining phalloidin-stained images to determine general features of cell shape for comparison between samples.

Electrical testing

Electrical testing was performed on day 3 for both static and strained constructs. A 2-point silver-chloride electrode was fabricated from silver sheeting, silver leads, a glass slide, and silicone insulation, as shown schematically in Figure 3A. Bioimpedance measurements were recorded using a Xitron 4000B bio-impedance spectrum analyzer (Xitron Technologies, San Diego, CA) over a logarithmic scale from 5 to 500 kHz. Constructs were removed from chamber wells still fixed to the polypropylene anchors and placed on an acrylic sheet, which provided a constant surface for electrode placement. Measurements were taken in paths perpendicular (longitudinal) and parallel (transverse) to the constrained axis or direction of ECM alignment [Fig. 3(B)]. Resistance, reactance, impedance, and phase of the samples were collected and conductivities were calculated using Ohm's law.

Statistics

All data presented is based on 4–6 independent experiments, each using a separate batch of collagen-fibrin-SWNT constructs. Statistical significance was analyzed using ANOVA with Tukey's test and a two-sample Student's t-test. Values of $p < 0.05$ were considered significant. Error bars on all graphs represent the standard error of the mean (SE).

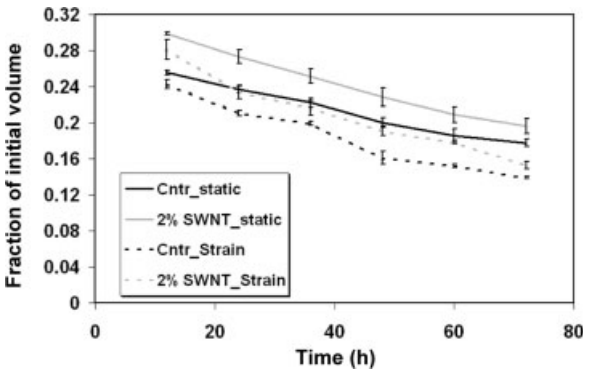

Figure 4. Gel compaction of CNTR and SWNT constructs under both static and strained conditions, over time in culture.

RESULTS

Cell-mediated gel compaction is a hallmark of these protein hydrogel constructs, as the embedded cells remodel and compact the matrix around them. Gel compaction proceeded steadily over the 3-day culture period in both static and strained constructs, as shown graphically in Figure 4. All samples compacted to less than 20% of their original volume by day 3. Control and 2 wt % SWNT constructs that underwent mechanical stimulation compacted significantly more than static constructs. No statistically significant difference in compaction was observed between control and 2 wt % constructs in either static or strained groups by day 3. However, the pattern of gel compaction varied between constructs cultured in static and dynamic environments, as shown in Figure 5. Static constructs maintained a constant rate of compaction over the 3 day period, with a slight decrease during the last 12 h [Fig. 5(A)]. Strained constructs exhibited higher rates of compaction during the period that they were exposed to strain, relative to the periods during which they were in static culture [Fig. 5(B)]. This phenomenon occurred in both control and 2 wt % constructs.

Images of HNDFb stained with a vital stain are shown in Figure 6 for each construct type (Panels A-D). Cell viability as quantified from confocal micrographs was consistently >90% in all samples [Fig. 6(E)], though mechanically stimulated control constructs exhibited slightly lower viability than all other samples. Cellular morphology was determined

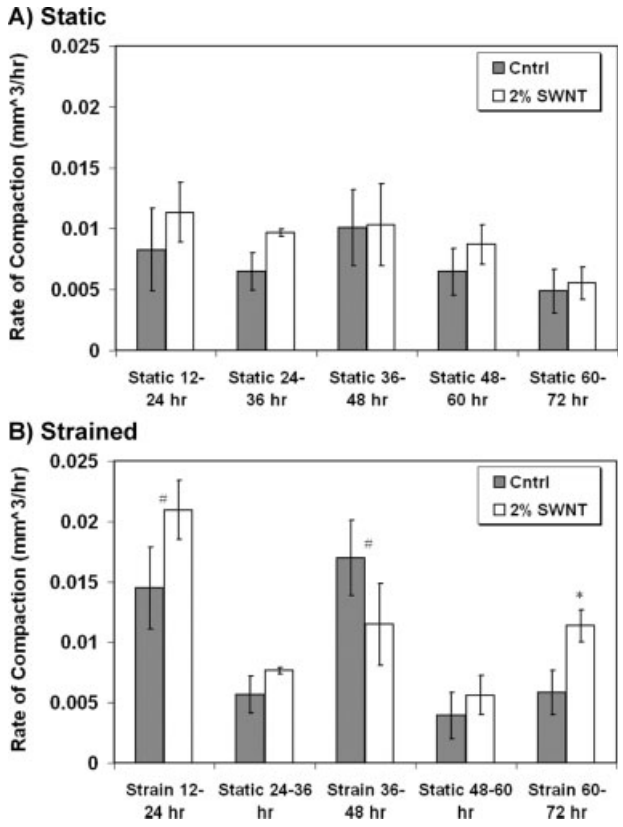

Figure 5. Rate of gel compaction expressed in 12-h intervals for static (A) and strained (B) constructs. Strained constructs were alternately cyclically stretched for 12-h, followed by 12 of unstretched culture. (# = statistically different from static; * = statistically different from control).

using fluorescent staining of the actin cytoskeleton of cells embedded in the 3-D matrix, as shown in Figure 7. Because of the effect of strained compaction, all constructs exhibited some degree of cell alignment in the longitudinal direction, however, this effect was more pronounced in strained constructs. Cells in static culture generally were more stellate with many multidirectional processes extending into the surrounding ECM. Static constructs with 2 wt % SWNT had fewer processes than controls but still maintained a typical star shaped morphology [Fig. 7(A,B)]. Cells in both control and 2 wt % SWNT strained constructs were characteristically spindle shaped [Fig. 7(C,D)].

Figure 8 shows SEM micrographs of SWNT-collagen-fibrin matrices. There were no observable morphological differences between control and 2 wt % SWNT constructs. The small size of SWNT is beyond the resolution capability of SEM, and even bundles were difficult to observe in such biological samples because of the incidence of charging at higher magnification, which obscured the image. Static cultures showed a random orientation of fibers with essentially isotropic structure [Fig. 8(A,B)]. Strained cultures showed fiber orientation parallel to the direction of stimulation [Fig. 8(C,D)]. Collagen fibers, which were distinguished by the characteristic banding pattern seen under SEM, were most prominently aligned in strained cultures with an underlying crosshatching of random fibrin fibers.

Bioimpedance measurements were used to calculate the conductivities of static and strained constructs as a function of AC frequencies. Figure 9 shows that conductivity values ranged from 1200–1600 mS/m depending on the type of construct and its culturing environment. Panel A shows frequency sweeps for static constructs, and panel B shows frequency sweeps for strained constructs. For statistical analysis, values from the frequency-independent range of 200–320 kHz were averaged, and these data are presented in Figure 10. Control constructs exhibited similar conductivities throughout all treatments: static and strained samples, in both transverse and longitudinal directions. The addition of SWNT to any construct significantly increased electrical conductivity in comparison with control constructs by an average of 95.6 $\pm$ 8.24 mS/m. Static samples containing SWNT did not exhibit statistically significant differences in conductivity depending on recording direction. However, mechanically strained samples with 2 wt % SWNT showed significantly increased conductivity in the longitudinal direction, compared with the transverse direction. The longitudinal conductivity of these strained SWNT-collagen-fibrin constructs also was statistically greater than all other SWNT-containing measurements, by an average of 122.2 $\pm$ 7.7 mS/m.

DISCUSSION

Our overall goal is to harness the high aspect ratio and electrical anisotropy of SWNT and similar nanofibers to create electrically conductive biopolymers. In particular, our aim in the present study was to use the well-established capability of fibroblast cells to remodel protein matrices to produce anisotropic tissue constructs with directional conductivity. This type of conduction-alignment relationship has been examined in other materials such as polymers and in highly concentrated SWNT scaffolds.[10,11] We chose to use biological polymers because of their self-assembly properties and cell compatibility. Our previous work examined several properties of collagen constructs containing SWNT, including cell proliferation, gel compaction, and electrical conductivity at different SWNT loadings.[23,24] We now have used active mechanical stimulation to align the matrix and create anisotropic composite biomaterials.

A main finding of this study was that strain-induced matrix alignment resulted in increased electrical conductivity along the aligned axis, but not

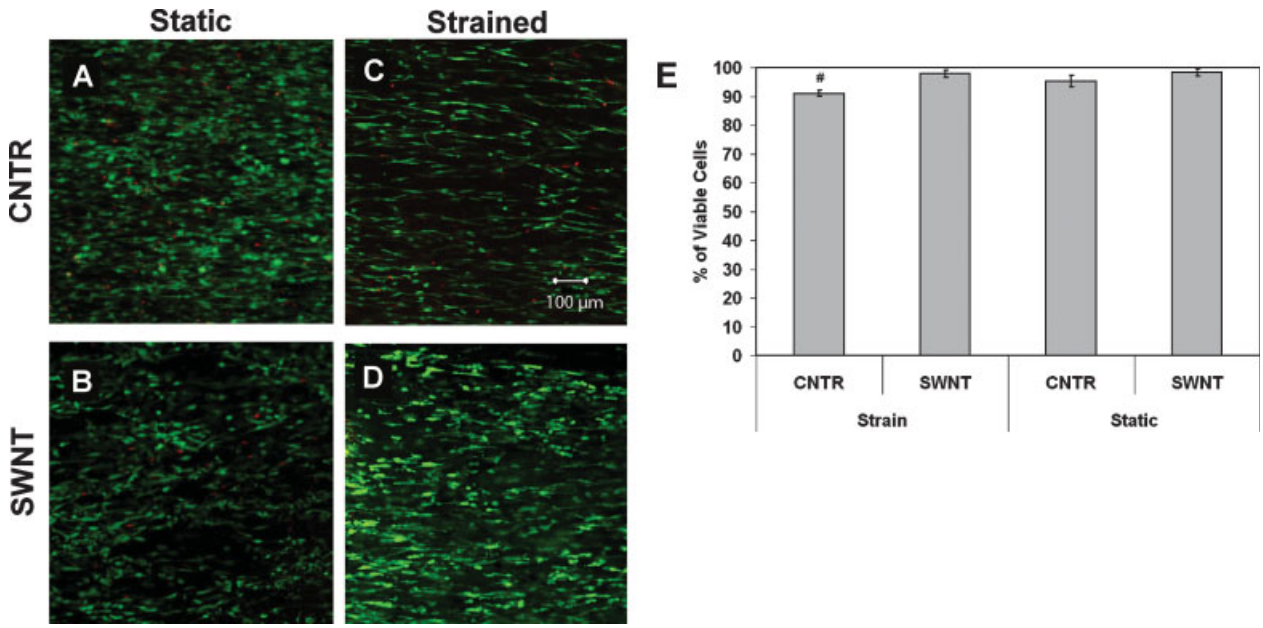

Figure 6. Confocal microscope images of HNDFb embedded in CNTR (A, C) and SWNT (B, D) constructs, under both static (A, B) and strained (C, D) conditions. Cells were stained with a vital dye and the percentage of living cells was determined using digital image analysis. Viability results are shown in panel E. (# = statistically different than other treatments). [Color figure can be viewed in the online issue, which is available at www.interscience.wiley.com.]

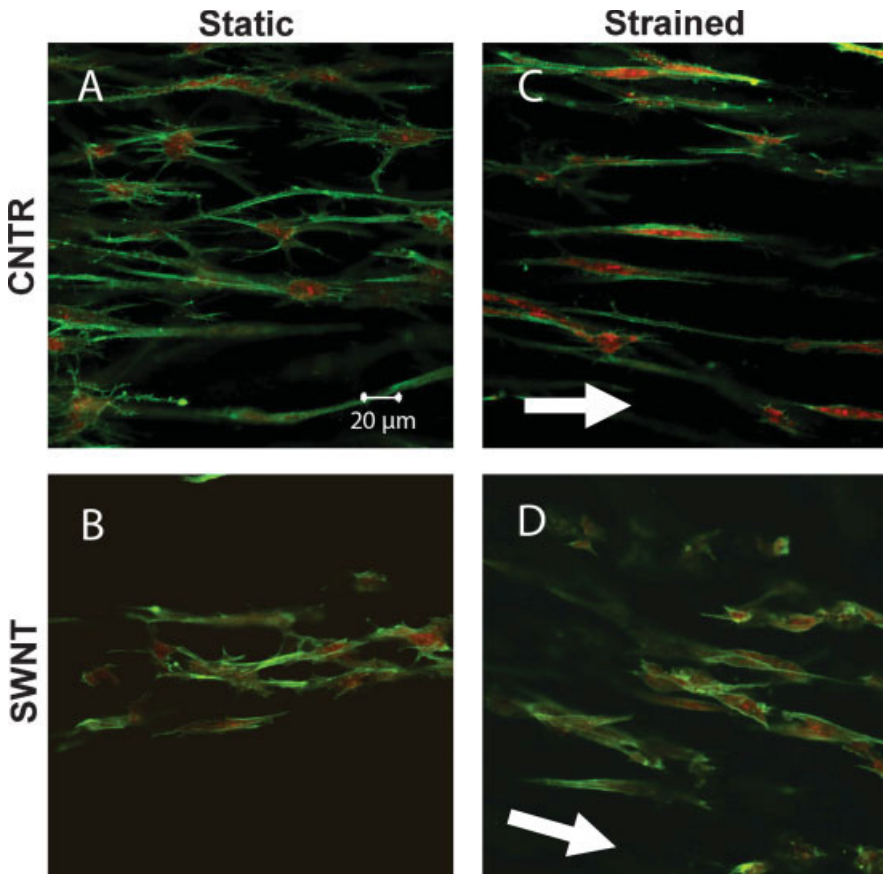

Figure 7. Confocal microscope images of HNDFb embedded in CNTR (A, C) and SWNT (B, D) constructs, under both static (A, B) and strained (C, D) conditions. The actin cytoskeleton and nucleus were stained in order to examine cell morphology and alignment. In the strained images, the arrow represents the direction of applied strain. [Color figure can be viewed in the online issue, which is available at www.interscience.wiley.com.]

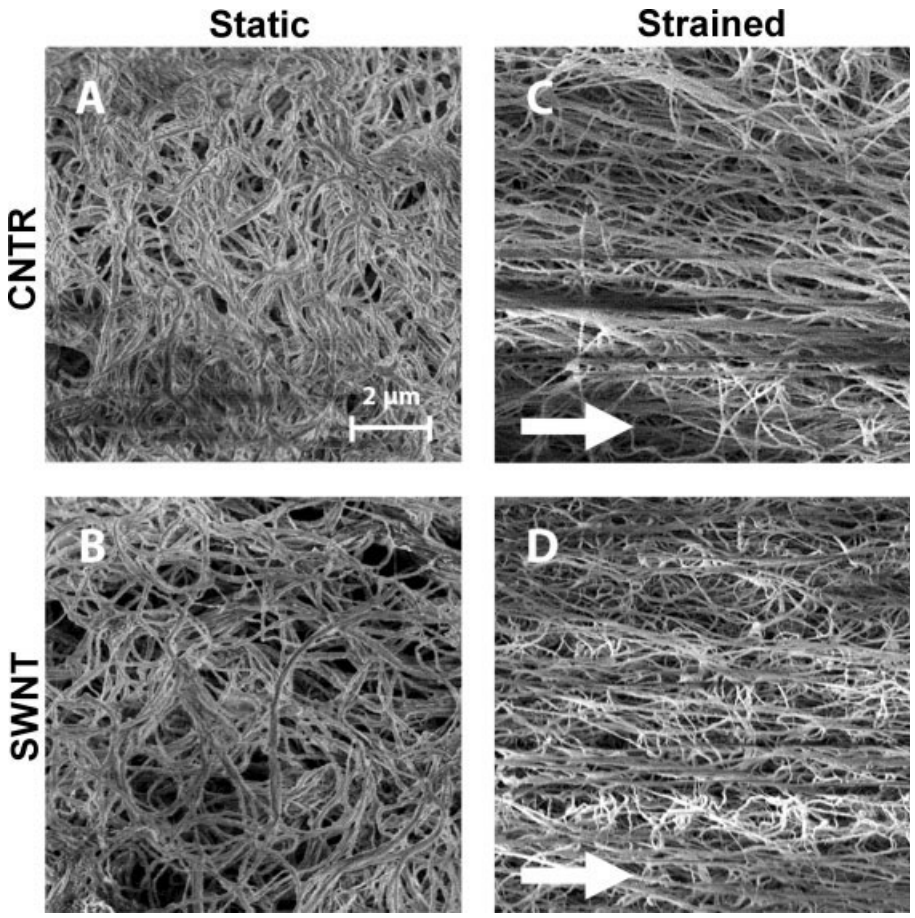

Figure 8. Scanning electron microscope images of CNTR (A, C) and SWNT (B, D) constructs, under both static (A, B) and strained (C, D) conditions. The collagen and fibrin matrix can be seen clearly. In the strained images, the arrow represents the direction of applied strain.

along the transverse axis of the constructs. As in our past work, there was a clear increase in conductivity when 2 wt % SWNT were added to the protein matrix, regardless of whether the sample was strained or not. However, in strained samples there was a pronounced additional conductivity increase along the longitudinal axis, suggesting that matrix and presumably SWNT alignment in that direction aided current flow. The results were highly reproducible and the increases resulting from both SWNT incorporation and strain alignment were statistically significant.

Cell-mediated compaction and remodeling of collagen gels is a well documented phenomenon that has been used to create a variety of engineered tissues. We added fibrin to our constructs because we have shown previously that this leads to a higher degree of compaction and more robust constructs.[12] In the present study, we observed robust gel compaction in both control and SWNT-loaded constructs to around 15–20% of their original volume. Application of mechanical strain increased the rate and degree of gel compaction. Furthermore, both constrained compaction and applied mechanical strain resulted in alignment of both the protein matrix and the embedded cells. Direct measurement of SWNT alignment in a protein matrix is experimentally very challenging; however, in the present study SWNT alignment could be inferred from matrix alignment and the increase in directional electrical properties. Nanotubes may be physically entrained during the protein polymerization process, and in addition there may be chemical interactions between the carboxylated SWNT and the protein molecules. In either case, one can expect that alignment of the protein matrix also would result in SWNT alignment.

The electrical conductivity increases we observed were clear, though modest in magnitude. The conductivity range of control constructs (i.e. no SWNT) was in the range of 1300–1350 mS/m, which agrees well with the 1300–1380 mS/m conductivity range published for culture medium alone.[25] The hydrogel constructs in this study contained a large fraction of water, and therefore in control constructs it is likely that current is being transported by the ionic medium. However, the increase in electrical conductivity that occurred when SWNT were added to the matrix suggests that in these constructs the compos-

ite material is carrying additional current. As we have observed in previous studies,[24] the electrical conductivity of cell-seeded CNT-protein hydrogels depends on the interrelated effects of SWNT loading and dispersion, gel compaction and SWNT alignment.

The SWNT used in this study were functionalized with carboxyl groups to facilitate their dispersion in aqueous medium.[26] The process of covalent functionalization introduces imperfections into the nanotube structure and also can lead to nanotube fragmentation.[27] These effects are likely to lower both the intrinsic electrical conductivity of SWNT as well as the likelihood of achieving electrical percolation (i.e. continuous current paths) through the material. In addition, currently available SWNT preparations contain both conductive and semi-conducting nanotubes. Each of these factors currently limits the degree to which SWNT loading can augment the electrical conductivity of materials, but advances in solubilization techniques[28,29] and separation methods[30,31] are likely to facilitate the creation of conductive composite materials using SWNT.

Nanotube functionalization also serves to greatly reduce the amount of metal catalyst and other impurities that are found in SWNT preparations, which is important in minimizing cellular toxicity.[32]

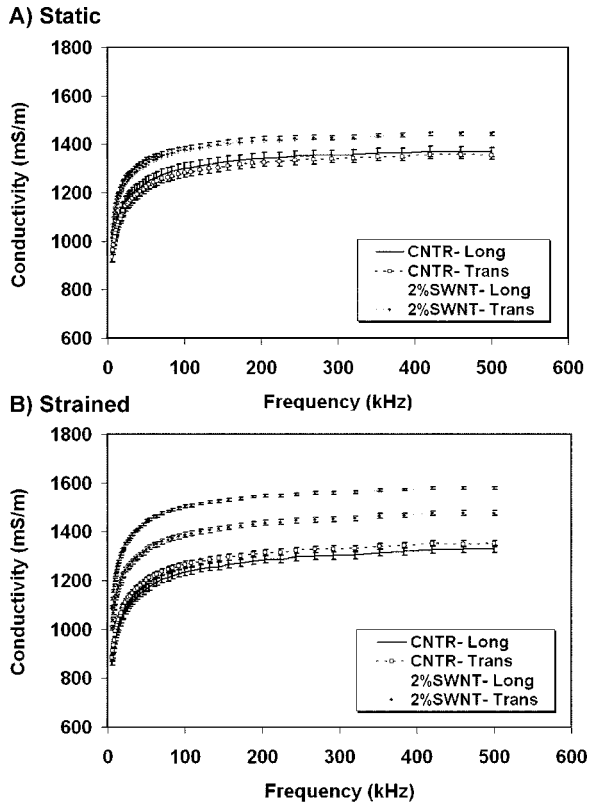

Figure 9. Electrical conductivity of static (A) and strained (B) CNTR and SWNT constructs, obtained by doing an AC frequency sweep and measuring bioimpedance.

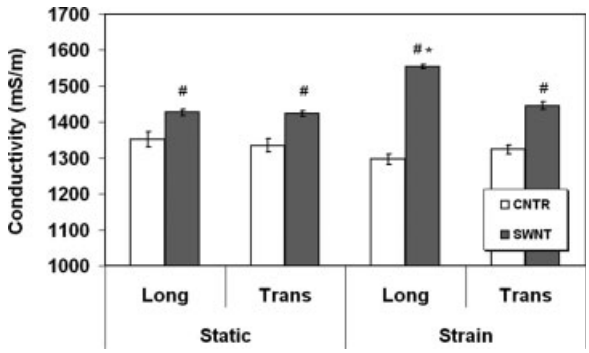

Figure 10. Electrical conductivity of static and strained CNTR and SWNT constructs. The presented values were obtained by averaging the values in the frequency-independent range (200–320 kHz). (# = statistically different from control; * = statistically different from transverse).

Our current results suggest that SWNT incorporation into 3D protein matrices did not significantly affect cell viability, morphology or cell-mediated gel compaction. The effects of nanotubes on cells, tissues and organisms is an area in need of greater investigation (for a recent review see e.g.[33]) and several groups have reported that SWNT dosage, aggregation, and functionalization may affect cellular activity.[34,35,36] In our current application, the cells are required mainly to compact and reorganize the protein matrix, in order to obtain directional anisotropy in the material. The cells in this study clearly retained these abilities.

Our work has demonstrated that SWNT can be used as a fibrous additive to 3D cell-seeded protein hydrogels, and that the SWNT serve to increase the electrical conductivity of such composite materials. Furthermore, the effect of SWNT loading can be enhanced by applying mechanical strain to the constructs, which induces the cellular component to align the matrix in a direction parallel to the applied strain. These anisotropic composite biomaterials are being developed for applications in which electrically conductive biopolymers may have utility, such as cardiac and neural tissue engineering, and biosensor development.

The authors thank Dr. Jonathon Newell and Dr. Tzu-Jen Kao for their help with electrical conductivity testing and analysis, and Matt Dalene for assistance with SEM and confocal imaging.

References

1. Williams D. Carbon nanotubes in medical technology. Med Device Technol 2007;18:8–10.
2. Goldberg M, Langer R, Jia X. Nanostructured materials for applications in drug delivery and tissue engineering. J Biomater Sci Polym Ed 2007;18:241–268.
3. Harrison BS, Atala A. Carbon nanotube applications for tissue engineering. Biomaterials 2007;28:344–353.

4. Haggenmuller R, Zhou W, Fischer JE, Winey KI. Production and characterization of polymer nanocomposites with highly aligned single-walled carbon nanotubes. J Nanosci Nanotechnol 2003;3:105–110.
5. Ayutsede J, Gandhi M, Sukigara S, Ye H, Hsu CM, Gogotsi Y, Ko F. Carbon nanotube reinforced Bombyx mori silk nanofibers by the electrospinning process. Biomacromolecules 2006; 7:208–214.
6. Giannona S, Firkowska I, Rojas-Chapana J, Giersig M. Vertically aligned carbon nanotubes as cytocompatible material for enhanced adhesion and proliferation of osteoblast-like cells. J Nanosci Nanotechnol 2007;7:1679–1683.
7. Meng J, Song L, Meng J, Kong H, Zhu G, Wang C, Xu L, Xie S, Xu H. Using single-walled carbon nanotubes nonwoven films as scaffolds to enhance long-term cell proliferation in vitro. J Biomed Mater Res A 2006;79:298–306.
8. Ajayan PM. Nanotubes from carbon. Chem Rev 1999;99:1787–1800.
9. Chang TE, Kisliuk A, Rhodes SM, Brittain WJ, Sokolov AP. Conductivity and mechanical properties of well-dispersed single-wall carbon nanotube/polystyrene composite. Polymer 2006;47:7740–7746.
10. Ma W, Song L, Yang R, Zhang T, Zhao Y, Sun L, Ren Y, Liu D, Liu L, Shen J others. Directly synthesized strong, highly conducting, transparent single-walled carbon nanotube films. Nano Lett 2007;7:2307–2311.
11. Bliznyuk VN, Singamaneni S, Sanford RL, Chiappetta D, Crooker B, Shibaev PV. Micro orientation and anisotropy of conductivity in liquid crystalline polymer films filled with carbon nanotubes. J Nanosci Nanotechnol 2005;5:1651–1655.
12. Cummings CL, Gawlitta D, Nerem RM, Stegemann JP. Properties of engineered vascular constructs made from collagen, fibrin, and collagen-fibrin mixtures. Biomaterials 2004;25: 3699–3706.
13. Rowe SL, Stegemann JP. Interpenetrating collagen-fibrin composite matrices with varying protein contents and ratios. Biomacromolecules 2006;7:2942–2948.
14. Costa KD, Lee EJ, Holmes JW. Creating alignment and anisotropy in engineered heart tissue: Role of boundary conditions in a model three-dimensional culture system. Tissue Eng 2003;9:567–577.
15. Shi Y, Vesely I. Fabrication of mitral valve chordae by directed collagen gel shrinkage. Tissue Eng 2003;9:1233–1242.
16. Girton TS, Barocas VH, Tranquillo RT. Confined compression of a tissue-equivalent: Collagen fibril and cell alignment in response to anisotropic strain. J Biomech Eng 2002;124:568–575.
17. Seliktar D, Nerem RM, Galis ZS. Mechanical strain-stimulated remodeling of tissue-engineered blood vessel constructs. Tissue Eng 2003;9:657–666.
18. Isenberg BC, Tranquillo RT. Long-term cyclic distention enhances the mechanical properties of collagen-based media-equivalents. Ann Biomed Eng 2003;31:937–949.
19. Ng CP, Swartz MA. Fibroblast alignment under interstitial fluid flow using a novel 3-D tissue culture model. Am J Physiol Heart Circ Physiol 2003;284:H1771–H1777.
20. Koster S, Leach JB, Struth B, Pfohl T, Wong JY. Visualization of flow-aligned type I collagen self-assembly in tunable pH gradients. Langmuir 2007;23:357–359.
21. Radisic M, Park H, Shing H, Consi T, Schoen FJ, Langer R, Freed LE, Vunjak-Novakovic G. Functional assembly of engineered myocardium by electrical stimulation of cardiac myocytes cultured on scaffolds. Proc Natl Acad Sci USA 2004;101:18129–18134.
22. Torbet J, Malbouyres M, Builles N, Justin V, Roulet M, Damour O, Oldberg A, Ruggiero F, Hulmes DJ. Orthogonal scaffold of magnetically aligned collagen lamellae for corneal stroma reconstruction. Biomaterials 2007;28:4268–4676.
23. MacDonald RA, Laurenzi BF, Viswanathan G, Ajayan PM, Stegemann JP. Collagen-carbon nanotube composite materials as scaffolds in tissue engineering. J Biomed Mater Res A 2005;74:489–496.
24. MacDonald RA, Voge C, Ajayan PM, Stegemann JP. Conductive biopolymers from collagen and carbon nanotubes. Forthcoming.
25. Mazzoleni AP, Sisken BF, Kahler RL. Conductivity values of tissue culture medium from 20 degrees C to 40 degrees C. Bioelectromagnetics 1986;7:95–99.
26. Peng H, Alemany LB, Margrave JL, Khabashesku VN. Sidewall carboxylic acid functionalization of single-walled carbon nanotubes. J Am Chem Soc 2003;125:15174–15182.
27. Wang Y, Iqbal Z, Mitra S. Rapidly functionalized, water-dispersed carbon nanotubes at high concentration. J Am Chem Soc 2006;128:95–99.
28. Karajanagi SS, Yang H, Asuri P, Sellitto E, Dordick JS, Kane RS. Protein-assisted solubilization of single-walled carbon nanotubes. Langmuir 2006;22:1392–1395.
29. Wang D, Chen L. Temperature and pH-responsive single-walled carbon nanotube dispersions. Nano Lett 2007;7:1480–1484.
30. Arnold MS, Green AA, Hulvat JF, Stupp SI, Hersam MC. Sorting carbon nanotubes by electronic structure using density differentiation. Nature Nanotechnology 2006;1:60–65.
31. Maeda Y, Kimura S, Kanda M, Hirashima Y, Hasegawa T, Wakahara T, Lian Y, Nakahodo T, Tsuchiya T, Akasaka T, Lu J, Zhang X, Gao Z, Yu Y, Nagase S, Kazaoui S, Minami N, Shimizu T, Tokumoto H, Saito R. Large-scale separation of metallic and semiconducting single-walled carbon nanotubes. J Am Chem Soc 2005;127:10287–10290.
32. Dillon AC, Yudasaka M, Dresselhaus MS. Employing Raman spectroscopy to qualitatively evaluate the purity of carbon single-wall nanotube materials. J Nanosci Nanotechnol 2004; 4:691–703.
33. Lam CW, James JT, McCluskey R, Arepalli S, Hunter RL. A review of carbon nanotube toxicity and assessment of potential occupational and environmental health risks. Crit Rev Toxicol 2006;36:189–217.
34. Raja PM, Connolley J, Ganesan GP, Ci L, Ajayan PM, Nalamasu O, Thompson DM. Impact of carbon nanotube exposure, dosage and aggregation on smooth muscle cells. Toxicol Lett 2007;169:51–63.
35. Wick P, Manser P, Limbach LK, Dettlaff-Weglikowska U, Krumeich F, Roth S, Stark WJ, Bruinink A. The degree and kind of agglomeration affect carbon nanotube cytotoxicity. Toxicol Lett 2007;168:121–131.
36. Nimmagadda A, Thurston K, Nollert MU, McFetridge PS. Chemical modification of SWNT alters in vitro cell-SWNT interactions. J Biomed Mater Res A 2006;76:614–625.